AAPT PHYSICS EDUCATION | AMERICAN JOURNAL of PHYSICS

Simulation of a Brownian particle in an optical trap

Giorgio Volpe and Giovanni Volpe

Citation: American Journal of Physics **81**, 224 (2013); doi: 10.1119/1.4772632
View online: http://dx.doi.org/10.1119/1.4772632
View Table of Contents: http://scitation.aip.org/content/aapt/journal/ajp/81/3?ver=pdfcov
Published by the American Association of Physics Teachers

COMPUTATIONAL PHYSICS

The Computational Physics Section publishes articles that help students and their instructors learn about the physics and the computational tools used in contemporary research. Most articles will be solicited, but interested authors should email a proposal to the editors of the Section, Jan Tobochnik (jant@kzoo.edu) or Harvey Gould (hgould@clarku.edu). Summarize the physics and the algorithm you wish to include in your submission and how the material would be accessible to advanced undergraduates or beginning graduate students.

Simulation of a Brownian particle in an optical trap

Giorgio Volpe
Institut Langevin, ESPCI ParisTech, CNRS UMR7587, 1 rue Jussieu, 75005 Paris, France

Giovanni Volpe[a)]
Physics Department, Bilkent University, Cankaya, 06800 Ankara, Turkey

(Received 8 October 2012; accepted 4 December 2012)

An optically trapped Brownian particle is a sensitive probe of molecular and nanoscopic forces. An understanding of its motion, which is caused by the interplay of random and deterministic contributions, can lead to greater physical insight into the behavior of stochastic phenomena. The modeling of realistic stochastic processes typically requires advanced mathematical tools. We discuss a finite difference algorithm to compute the motion of an optically trapped particle and the numerical treatment of the white noise term. We then treat the transition from the ballistic to the diffusive regime due to the presence of inertial effects on short time scales and examine the effect of an optical trap on the motion of the particle. We also outline how to use simulations of optically trapped Brownian particles to gain understanding of nanoscale force and torque measurements, and of more complex phenomena, such as Kramers transitions, stochastic resonant damping, and stochastic resonance.
[http://dx.doi.org/10.1119/1.4772632]

I. INTRODUCTION

Randomness is present in most phenomena, ranging from biomolecules and nanodevices to financial markets and human organizations.[1] It is not easy to gain an intuitive understanding of stochastic phenomena, because their modeling typically requires advanced mathematical tools. A good pedagogical approach is to start with some simple stochastic systems. Experience can be gained by doing numerical experiments, which are inexpensive and within the reach of students with access to a computer.

One of the simplest examples of a stochastic system is a Brownian particle, which is a microscopic particle suspended in a fluid.[2] Brownian particles are often used to study random phenomena, because their motion due to thermal agitation from collisions with the surrounding fluid molecules provides a well-defined random background dependent on the temperature and the fluid viscosity.[3] By introducing optical forces to induce deterministic perturbations on the particles,[4] it is possible to study the interplay between random and deterministic forces. Optically trapped particles have been used as a model system for statistical physics, and have a wide range of applications, including, for example, the measurement of nanoscopic forces[5–8] and torques.[9–11]

The motion of an optically trapped Brownian particle in one dimension can be modeled by the Langevin equation

$$\underbrace{m\ddot{x}(t)}_{\text{inertia}} = \underbrace{-\gamma\dot{x}(t)}_{\text{friction}} + \underbrace{kx(t)}_{\text{restoring force}} + \underbrace{\sqrt{2k_BT\gamma}\,W(t)}_{\text{white noise}}, \tag{1}$$

where x is the particle position, m is its mass, γ is the friction coefficient, k is the trap stiffness, $\sqrt{2k_BT\gamma}\,W(t)$ the fluctuating force due to random impulses from the many neighboring fluid molecules, k_B is Boltzmann's constant, and T is the absolute temperature. Equation (1) is an example of a stochastic differential equation,[12] a common tool used to describe stochastic phenomena and is obtained by the addition of a white noise term to an ordinary differential equation (ODE) describing an overdamped harmonic oscillator.

Unlike ODEs, which are routinely taught in undergraduate courses, stochastic differential equations are complex, mostly because the white noise is almost everywhere discontinuous and has infinite variation.[12] The numerical integration of stochastic differential equations requires advanced mathematical tools, such as σ-algebras, the Itô formula, and martingales,[12] which are far beyond the level of most undergraduate courses. The numerical solution of stochastic differential equations is usually not straightforward.[13]

In the following, we will explain how to solve Eq. (1) numerically using a simple finite difference algorithm. First, we will explain how to simulate a random walk and, in particular, how to treat the white noise term within a finite difference framework. We will then describe how to simulate the free diffusion of a Brownian particle and study its transition from the ballistic to the diffusive regime due to the presence of inertial effects at short time scales. Subsequently, we will examine the effect of the optical trap on the motion of the particle. Finally, we will give some suggestions on how to simulate the behavior of an optically trapped particle in the presence of external forces or torques, and on how to employ optically trapped Brownian particles to address more complex phenomena, such as Kramers transitions,[14] stochastic resonant damping,[15] and stochastic resonance.[16]

Simulations can also complement the use of optical tweezers in undergraduate laboratories.[17–19] The associated MATLAB programs are freely available.[20] These MATLAB programs can be straightforwardly adapted to the freeware SCILAB.[21]

II. SIMULATION OF WHITE NOISE

Finite difference simulations of ODEs are straightforward: the continuous-time solution $x(t)$ of an ODE is approximated by a discrete-time sequence x_i, which is the solution of the corresponding finite difference equation evaluated at regular time steps $t_i = i\Delta t$. If Δt is sufficiently small, $x_i \approx x(t_i)$. A finite difference equation is obtained from the ODE by replacing $x(t)$ by x_i, $\dot{x}(t)$ by $(x_i - x_{i-1})/\Delta t$, and $\ddot{x}(t)$ by

$$\frac{(x_i - x_{i-1})/\Delta t - (x_{i-1} - x_{i-2})/\Delta t}{\Delta t} = \frac{x_i - 2x_{x-1} + x_{i-2}}{\Delta t^2}. \tag{2}$$

The solution is obtained by solving the resulting finite difference equation recursively for x_i, using the values x_{i-1} and x_{i-2} from previous iterations. This first-order integration method generalizes the Euler method to stochastic differential equations. Higher-order algorithms can also be employed to obtain faster convergence of the solution.[13]

All the terms in Eq. (1) can be approximated as we have described except for the white noise term $W(t)$. $W(t)$ is characterized by the following properties:[12] the mean $\langle W(t)\rangle = 0$ for all t; $\langle W(t)^2\rangle = 1$ for each value t; and $W(t_1)$ and $W(t_2)$ are independent of each other for $t_1 \neq t_2$. Because of these properties, white noise cannot be treated as a standard function. In particular, it is almost everywhere discontinuous and has infinite variation. Thus, it cannot be approximated by its instantaneous values at times t_i, because these values are not well-defined (due to the lack of continuity) and their magnitude varies wildly (due to the infinite variation).

To understand how to treat $W(t)$ within a finite difference approach, consider the equation

$$\dot{x}(t) = W(t), \tag{3}$$

which is the simplest version of a free diffusion equation and whose solution is usually called a *random walk*. We need a discrete sequence of random numbers W_i that mimics the properties of $W(t)$. Because $W(t)$ is stationary with zero mean, W_i are random numbers with zero mean. We also impose the condition that $\langle (W_i\Delta t)^2\rangle/\Delta t = 1$ so that the W_i have variance $1/\Delta t$, where $\langle\cdots\rangle$ represents an ensemble average. Because $W(t)$ is uncorrelated, we assume W_i and W_j to be independent for $i \neq j$; that is, we use a sequence of uncorrelated random numbers with zero mean and variance $1/\Delta t$. Some languages have built in functions that directly generate a sequence w_i of Gaussian random numbers with zero mean and unit variance. Alternatively, it is possible to employ various algorithms to generate Gaussian random numbers using uniform random numbers between 0 and 1, such as the Box-Muller algorithm or the Marsaglia polar algorithm.[13] We then rescale w_i to obtain the sequence $W_i = w_i/\sqrt{\Delta t}$ with variance $1/\Delta t$. Figures 1(a)–1(c) show how the values of W_i increase and diverge as $\Delta t \to 0$.

The finite difference equation corresponding to Eq. (3) is

$$\frac{x_i - x_{i-1}}{\Delta t} = \frac{w_i}{\sqrt{\Delta t}}, \tag{4}$$

or

$$x_i = x_{i-1} + \sqrt{\Delta t}\, w_i. \tag{5}$$

Some examples of the resulting free diffusion trajectories x_i are plotted (lines) in Figs. 1(d)–1(f) for $\Delta t = 1.0$, 0.5, and 0.1, respectively. The numerical solutions become more jagged as Δt decreases. The solutions shown in Figs. 1(d)–1(f) differ because they are specific realizations of a random process, but their statistical properties do not change, as can be seen by averaging over many realizations. The shaded areas in Figs. 1(d) and 1(f), which represent the variance around the mean position of the freely diffusing random walker obtained by averaging over 10,000 trajectories, are roughly the same, independent of Δt. (The small differences are due to the finite number of trajectories used in the averaging.)

The time step Δt should be much smaller than the characteristic time scales of the stochastic process to be simulated. If Δt is comparable to or larger than the smallest time scale, the numerical solution will not converge and typically shows

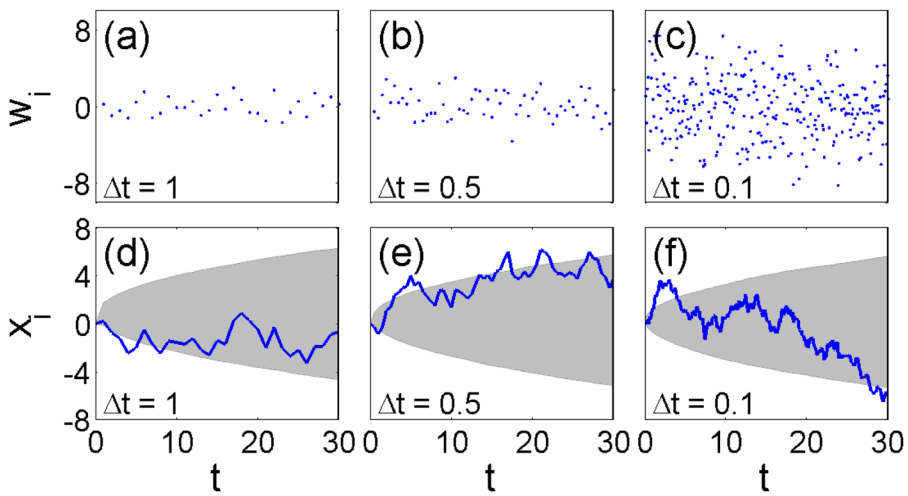

Fig. 1. As the time step Δt decreases, we must employ larger values of the Gaussian white noise W_i to approximate the solution of the free diffusion equation [Eq. (3)] accurately. (a) $\Delta t = 1$, (b) 0.5, and (c) 0.1. The corresponding solutions of the finite difference free diffusion equation [Eq. (5)] in (d)–(f) for x_i (lines) behave similarly. Although these solutions differ because they are specific realizations of a random process, their statistical properties do not change, as can be seen by comparing the shaded areas, which show the regions within one standard deviation of the mean of 10,000 realizations.

an unphysical oscillatory behavior or divergence. The case of free diffusion treated in this section is special because there is no characteristic time scale, as can be seen from the fact that Eq. (3) is self-similar under a rescaling of the time, and therefore there is no optimal choice of Δt.

III. FROM BALLISTIC MOTION TO BROWNIAN DIFFUSION

We now consider the Brownian motion of real particles. A microscopic particle immersed in a fluid undergoes *diffusion* because of the collisions with the surrounding fluid molecules such that each collision alters the velocity of the particle, which then drifts in a random direction until the next collision. After a large number of such events the direction and speed of the particle are effectively randomized. These collisions also limit the particle's average kinetic energy to $k_BT/2$ for each degree of freedom in accordance with the equipartition theorem.[22] The diffusion and friction coefficients, D and γ, respectively, are closely related to the average kinetic energy by the Einstein relation $\gamma D = k_BT$. The Langevin equation describing the resulting motion is Eq. (1) without the force term:

$$m\ddot{x}(t) = -\gamma\dot{x}(t) + \sqrt{2k_BT\gamma}\,W(t). \tag{6}$$

Equation (6) can be solved numerically by considering the corresponding finite difference equation,

$$m\frac{x_i - 2x_{i-1} + x_{i-2}}{(\Delta t)^2} = -\gamma\frac{x_i - x_{i-1}}{\Delta t} + \sqrt{2k_BT\gamma}\frac{1}{\sqrt{\Delta t}}\eta_i. \tag{7}$$

The solution for x_i is

$$x_i = \frac{2 + \Delta t(\gamma/m)}{1 + \Delta t(\gamma/m)}x_{i-1} - \frac{1}{1 + \Delta t(\gamma/m)}x_{i-2} + \frac{\sqrt{2k_BT\gamma}}{m[1 + \Delta t(\gamma/m)]}(\Delta t)^{3/2}w_i. \tag{8}$$

The ratio $\tau = m/\gamma$ is the momentum relaxation time—the time scale of the transition from smooth ballistic behavior to diffusive behavior. The time τ is very small, typically on the order of a few nanoseconds.[2,23]

We will consider a silica microparticle in water with radius $R = 1\,\mu$m, mass $m = 11$ pg, viscosity $\eta = 0.001\,\mathrm{Ns/m^2}$, $\gamma = 6\pi\eta R$, temperature $T = 300$K, and $\tau = 0.6\,\mu$s. We remark that τ is orders of magnitude smaller than the time scales of typical experiments. Only since 2010 has it been possible to experimentally measure the particle position sufficiently fast to probe its instantaneous velocity and the transition from the ballistic to the diffusive regime.[24] Thus, it is often possible to drop the inertial term (i.e., set $m = 0$) and obtain from Eq. (6)

$$\dot{x}(t) = \sqrt{2D}\,W(t). \tag{9}$$

In terms of the finite differences, Eq. (9) becomes

$$x_i = x_{i-1} + \sqrt{2D\Delta t}\,w_i. \tag{10}$$

Equation (10) is a very good approximation to Brownian motion for long time steps ($\Delta t \gg \tau$) but it shows clear deviations at short time scales ($\Delta t \lesssim \tau$). In Figs. 2(a) and 2(b), we compare two trajectories with and without inertia using the same realization of the white noise. For short times [see Fig. 2(a)], the trajectory of a particle with inertia (solid line) appears smooth with a well-defined velocity which also changes smoothly, while in the absence of inertia (dashed line) the trajectory is ragged and discontinuous with a velocity which is not well-defined. Note how the non-inertial trajectory changes direction at every time step and appears to be a series of broken line segments, while the inertial trajectory is smooth. For long times [see Fig. 2(b)] both the trajectory with inertia (solid line) and without inertia (dashed line) show behavior typical of the diffusion of a Brownian particle—they appear jagged because the microscopic details are not resolvable.

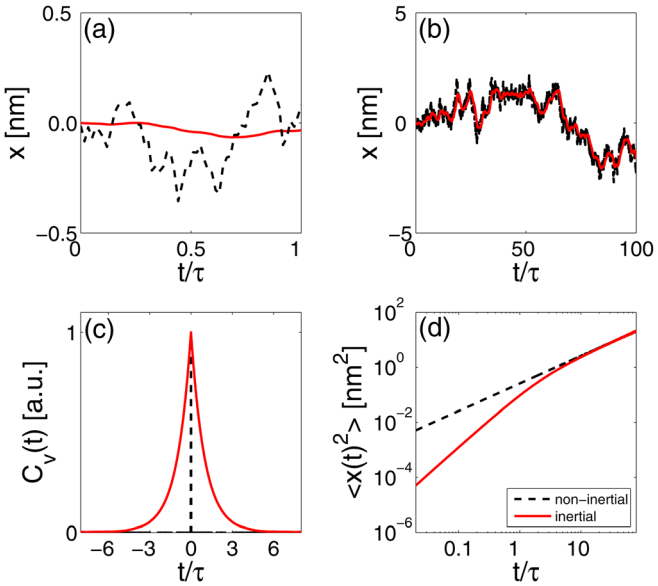

Fig. 2. (a) For times smaller or comparable to the inertial time τ the trajectory of a particle with inertia (solid line) appears smooth. In contrast, in the absence of inertia (dashed line) the trajectory is ragged and discontinuous. (b) For times significantly longer than τ both the trajectory with inertia (solid line) and without inertia (dashed line) are jagged, because the microscopic details are not resolvable. These trajectories are computed using Eqs. (8) and (10) with $\Delta t = 10$ ns and the same realization of the white noise so that the two trajectories can be compared. (c) The velocity autocorrelation function [Eq. (12)] for a particle with inertia (solid line) decays to zero with the time constant τ, while for a particle without inertia (dashed line) it drops immediately to zero demonstrating that its velocity is not correlated and does not have a characteristic time scale. (d) A log-log plot of the mean-square displacement [Eq. (14)] for a particle with inertia (solid line) shows a transition from quadratic behavior at short times to linear behavior at long times, while for a particle without inertia (dashed line) it is always linear. The particle parameters are $R = 1\,\mu$m, $m = 11$ pg, $\eta = 0.001\,\mathrm{Nsm^{-2}}$, $\gamma = 6\pi\eta R$, $T = 300$K, and $\tau = m/\gamma = 0.6\,\mu$s are used here and for the numerical solutions shown in the following figures.

To better understand the free diffusion of a Brownian particle and the differences between the inertial and non-inertial regimes, we analyze some statistical quantities that are derived from the trajectories, namely, the velocity autocorrelation function and the mean square displacement of the particle position. The velocity autocorrelation function provides a measure of the time it takes for the particle to "forget" its initial velocity and is defined as

$$C_v(t) = \overline{v(t' + t)v(t')}, \tag{11}$$

where the bar represents a time average. From the simulations C_v becomes the discrete function

$$C_{v,n} = \overline{v_{i+n} v_i}, \tag{12}$$

where $v_i = (x_{i+1} - x_i)/\Delta t$. The solid line in Fig. 2(c) depicts the velocity autocorrelation function for a Brownian particle with inertia and shows that $C_v(t)$ decays to zero with the time constant τ, demonstrating the time scale over which the velocity of the particle becomes uncorrelated with its initial value. The dashed line in Fig. 2(c) represents $C_v(t)$ for a trajectory without inertia, which drops immediately to zero demonstrating that, in the absence of inertia, the velocity is uncorrelated over all times and thus does not have a characteristic time scale.

The mean square displacement quantifies how a particle moves from its initial position. For ballistic motion, the mean square displacement is proportional to t^2, and for diffusive motion it is proportional to t.[24] The mean square displacement is defined as

$$\langle x(t)^2 \rangle = \overline{[x(t'+t) - x(t')]^2} \tag{13}$$

and can be calculated from a trajectory as

$$\langle x_n^2 \rangle = \overline{[x_{i+n} - x_i]^2}. \tag{14}$$

The fact that the ensemble average and the time average coincide is a consequence of the ergodicity of the system. The solid line in Fig. 2(d) shows the mean square displacement in the presence of inertia. At short times $(t \lesssim \tau)$ $\langle x(t)^2 \rangle$ is quadratic in t, and for longer times $(t \gg \tau)$ $\langle x(t)^2 \rangle$ becomes linear. This transition from ballistic to diffusive motion occurs on a time scale τ. In the absence of inertia (dashed line), $\langle x(t)^2 \rangle$ is always linear.

IV. OPTICAL TRAPS

In many cases, it is useful to hold some Brownian particles in place. In this way, for example, it is possible to study the physical and chemical properties of cells and biomolecules[8] and to use inert microscopic particles as force nanotransducers.[25] One of the most effective ways of holding Brownian particles is by means of *optical traps*, or *optical tweezers*.[4] An optical trap is formed in the proximity of the focal spot of a highly focused laser beam and is due to the momentum transfer from the light to the particle. Because the light is bent when it passes through the particle, it experiences a change in its momentum and therefore produces a recoil of the particle. Under the appropriate conditions, the particle can be trapped in three dimensions as the focused laser beam produces three independent harmonic traps in the three orthogonal spatial directions.[26]

A Brownian particle in an optical trap is in dynamic equilibrium with the thermal noise pushing it out of the trap and the optical forces driving it toward the center of the trap. The time scale on which the restoring force acts is given by the ratio $\phi = \gamma/k$ and is typically much greater than τ. To study the dynamics of the Brownian particle in the trap, it is often convenient to employ the non-inertial approximation to Brownian motion so that the only relevant time scale is ϕ, so that we can employ a relatively large time step $\Delta t > \tau$. The time step Δt should still be significantly smaller than ϕ, because, if $\Delta t \gtrsim \phi$, the numerical solution does not converge and typically shows an unphysical oscillatory behavior or divergence. We encourage readers to explore the numerical solutions for this case to see what happens.

The motion of the particle is described by a set of three independent Langevin equations such as Eq. (1), where the inertial term is dropped (i.e., $m = 0$). This equation can be written as

$$\dot{\vec{r}}(t) = -\frac{1}{\gamma} \vec{k} \cdot \vec{r}(t) + \sqrt{2D}\, \vec{W}(t), \tag{15}$$

where $\vec{r} = [x, y, z]$ represents the position of the particle, $\vec{k} = [k_x, k_y, k_z]$ is the stiffnesses of the trap, and $\vec{W} = [W_x, W_y, W_z]$ is a vector of white noise. The corresponding finite difference equation is

$$\vec{r}_i = \vec{r}_{i-1} - \frac{1}{\gamma} \vec{k} \cdot \vec{r}_{i-1} \Delta t + \sqrt{2D\Delta t}\, \vec{w}_i, \tag{16}$$

where $\vec{r}_i = [x_i, y_i, z_i]$ represents the position of the particle at time t_i and $\vec{w}_i = [w_{i,x}, w_{i,y}, w_{i,z}]$ is a vector of Gaussian random numbers with zero mean and unit variance.

The line in Fig. 3(a) shows a simulated trajectory of a Brownian particle in an optical trap with $k_x = k_y = 1.0 \times 10^{-6}$ fN/nm and $k_z = 0.2 \times 10^{-6}$ fN/nm, where $1\,\text{fN} = 10^{-15}$ N. The fact that the trapping stiffness along the beam propagation axis (z) is smaller than in the perpendicular plane is commonly observed in experiments and is due to the presence of scattering forces along z.[26] Thus, the particle explores an ellipsoidal volume around the center of the trap, as shown by the shaded area, which represents an equiprobability surface. In Figs. 3(b) and 3(c), we show the probability distribution of finding the particle in the z- and y-planes, respectively.

It is possible to increase the stiffness of the trap by increasing the optical power, thereby improving the confinement of the particle.[27] The stiffness can be quantified by measuring the variance σ_{xy}^2 of the particle position around the trap center in the y-plane. In Fig. 4(a), the variance σ_{xy}^2 is shown as a function of k_x. It is seen that $\sigma_{xy}^2 \propto 1/k_{xy}$. In Figs.

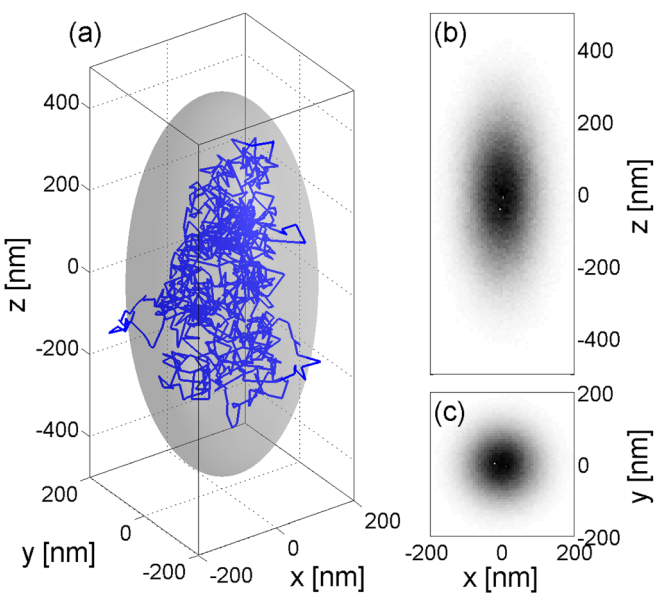

Fig. 3. (a) Trajectory of a Brownian particle in an optical trap ($k_x = k_y = 1.0 \times 10^{-6}$ fN/nm and $k_z = 0.2 \times 10^{-6}$ fN/nm). The particle explores an ellipsoidal volume around the center of the trap, as evidenced by the shaded area which represents an equiprobability surface. (b) and (c) The probability distributions of finding the particle in the z- and y-planes follow a two-dimensional Gaussian distribution around the trap center.

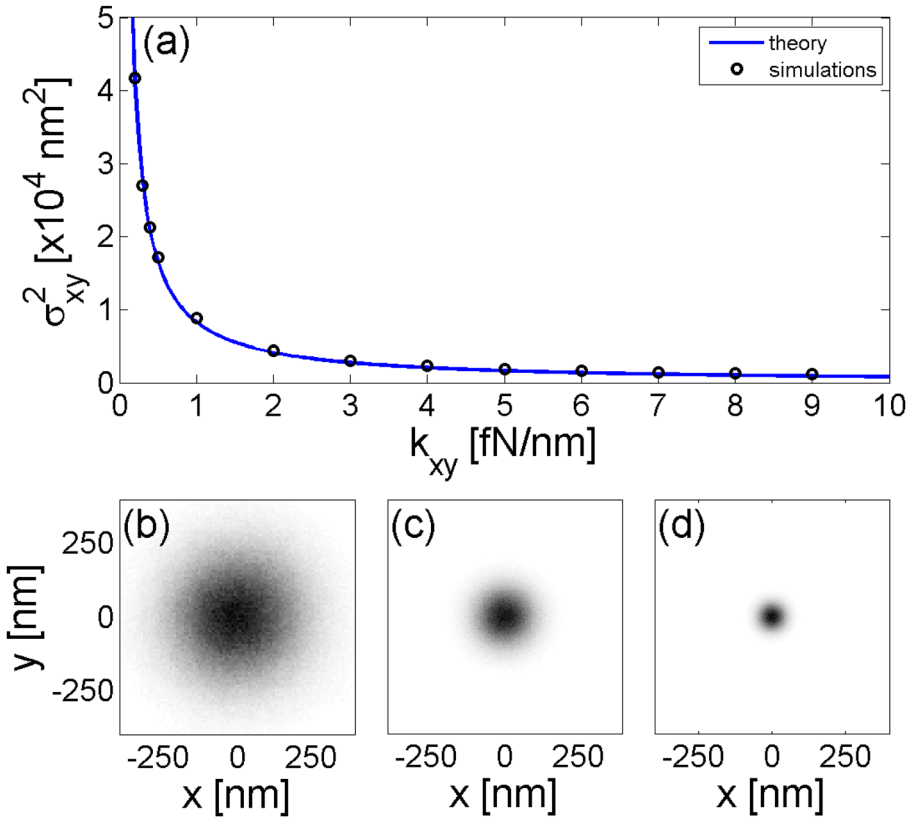

Fig. 4. (a) As the trap stiffness k_{xy} increases, the particles become more and more confined as shown by the theoretical (solid curve) and numerical (symbols) variance σ_{xy} of the particle position around the trap center in the y-plane and, in particular, by the probability distributions corresponding to (b) $k_{xy} = 0.2\,\mathrm{fN/nm}$, (c) $k_{xy} = 1.0\,\mathrm{fN/nm}$, and (d) $k_{xy} = 5.0\,\mathrm{fN/nm}$.

4(b)–4(d), the position distributions in the y-plane are observed to shrink as the stiffness is increased.

The time scale ϕ, which characterizes how the particles fall into the trap, can be seen in the position autocorrelation function [see Fig. 5(a)]

$$C_x(t) = \overline{x(t'+t)x(t')}. \tag{17}$$

As the stiffness increases, the particle undergoes a stronger restoring force and the correlation time decreases, because the particle explores a smaller phase-space. Unlike the free diffusion case, the mean square displacement [see Fig. 5(b)] does not increase indefinitely but reaches a plateau because of the confinement imposed by the trap. The transition from the linear growth corresponding to the free diffusion behavior and the plateau due to the confinement occurs at about ϕ.

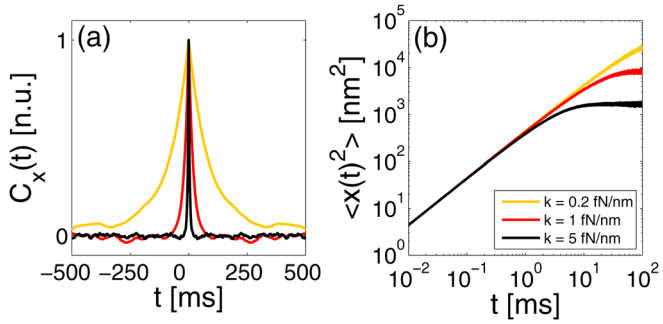

Fig. 5. (a) The position autocorrelation function of a trapped particle [Eq. (23)] gives information about the effect of the trap restoring force on the particle motion. As the trap stiffness and, therefore, the restoring force are increased, the characteristic decay time of the position autocorrelation function decreases. (b) The mean square displacement, unlike for the free diffusion case, does not increase indefinitely but reaches a plateau, which also depends on the trap stiffness—the stronger the trap, the sooner the plateau is reached.

V. FURTHER NUMERICAL EXPERIMENTS

By following the approach we have discussed, readers can study other phenomena where more complex forces act on the particle. Equation (1) can be generalized to

$$\dot{x}(t) = \frac{1}{\gamma}F(x(t),t) + \sqrt{2D}\,W(t), \tag{18}$$

where $F(x(t), t)$ represents a force acting on the particle that can vary both in space and time. For example, for a simple optical trap, $F(x(t), t) = -kx(t)$, and we obtain Eq. (1).

We now consider one of the simplest cases and add a constant force F_c that acts on the particle from time $t = 0$, that is, $F(x(t),t) = -kx(t) + F_c(t)\,h(t)$ where $h(t)$ is the Heaviside step function. This force results in a shift of the equilibrium position of the particle within the trap, as shown in Fig. 6(a), where the probability distribution of the particle for $t < 0$ is represented by the black histogram and the one for $t > 0$ by the grey histogram. By measuring the shift of the average position Δx and using the knowledge of k, it is possible to measure $F_c = k\Delta x$ (Hooke's law). This experimental technique, known as photonic force microscopy, has been widely employed to measure nanoscopic forces exerted by biomolecules.[25]

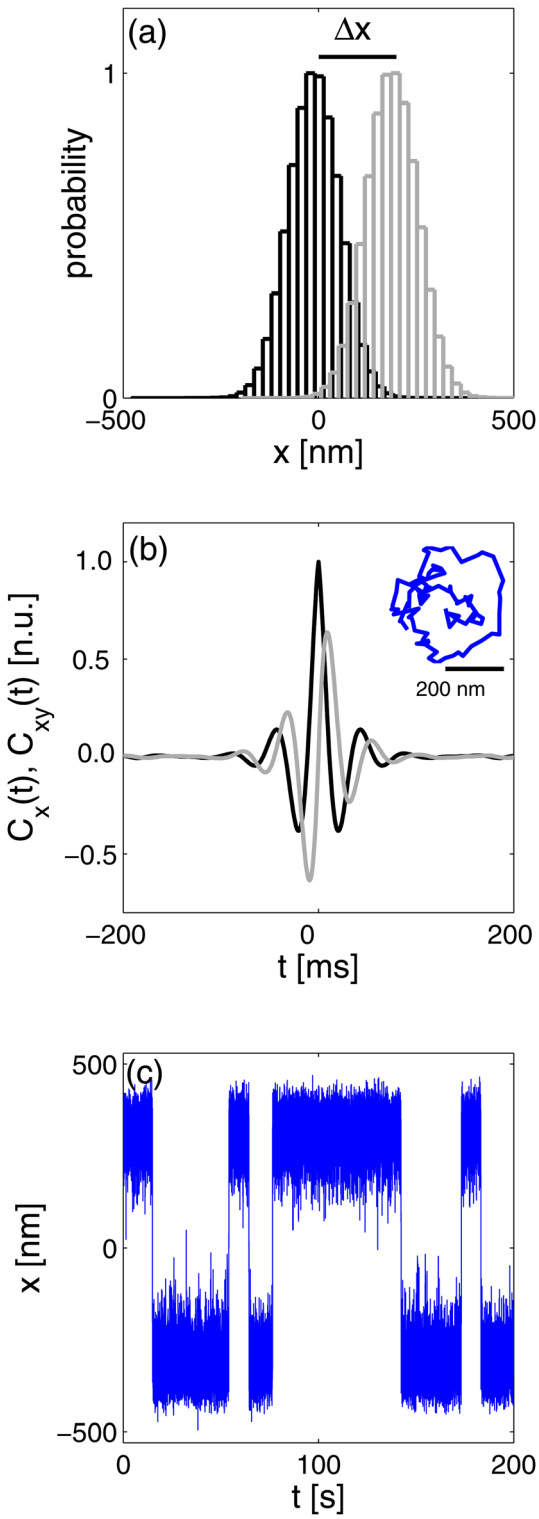

Fig. 6. (a) The probability distribution of an optically trapped particle shifts in response to an external force. The black histogram shows the initial distribution and the grey histogram represents the distribution after the application of a constant external force $F_c = 200\,\text{fN}$. (b) The position autocorrelation function of the trapped particle [black line, Eq. (23)] and position cross-correlation function [grey line, Eq. (20)], are modulated in the presence of a rotational force field such as the one in Eq. (19) with $\Omega = 132.6\,\text{s}^{-1}$. This modulation demonstrates the presence of the rotational force field even though it is not clear from the trajectory (the inset shows a trajectory during a time interval equal to 0.1 s). (c) Dynamic transitions between the two equilibrium positions in a double-well potential (Kramers transitions) with $a = 1.0 \times 10^7\,\text{N/m}^3$ and $b = 1.0 \times 10^{-6}\,\text{N/m}$ [Eq. (21)].

It is possible to introduce non-conservative forces in two dimensions. The simplest case is a simple rotational force field such as

$$\vec{F}(x,y) = -\begin{bmatrix} k & \gamma\Omega \\ -\gamma\Omega & k \end{bmatrix}\begin{bmatrix} x \\ y \end{bmatrix}, \tag{19}$$

where Ω represents the rotational component. It is interesting to see how the motion of the particle changes from a situation where the rotation is clearly visible for large Ω to a situation where it is hardly visible for small Ω. An intermediate situation is plotted by the line in the inset in Fig. 6(b).[7,11,28,29] Such a force induces a cross-correlation between the motion in the x- and y-directions [black line in Fig. 6(b)], defined by

$$C_{xy}(t) = \overline{x(t'+t)y(t')}. \tag{20}$$

As the particle moves (on average) around the origin, $C_{xy}(t)$ oscillates [grey line in Fig. 6(b)].

It is also possible to study several statistical phenomena. For example, consider a double-well potential such as $U(x) = ax^4/4 - bx^2/2$, which produces the force

$$F(x) = -ax^3 + bx. \tag{21}$$

Such a force has been experimentally realized using two close optical traps.[14] There are two equilibrium positions located at the potential minima and separated by a potential barrier between which the Brownian particle can jump (Kramers transitions), as shown by the trajectory shown in Fig. 6(c). Readers can explore the statistics of the residence times in the two potential wells and their variation as a function of the height of the potential barrier and the temperature. As the potential barrier decreases and/or the temperature increases, the jumps become more frequent. Because the double-well potential is symmetric, the residence times are equal for the two equilibrium positions. Another interesting problem is to study how the residence times vary in an asymmetric potential well, which can be obtained by adding a constant force to Eq. (21).

It also is possible to introduce time-varying potentials and study phenomena such as stochastic resonant damping and stochastic resonance. Stochastic resonant damping[15] occurs as the equilibrium position of a harmonic trap is made to oscillate with a frequency f and an amplitude x_c, such that

$$F(x(t),t) = -k[x(t) - x_c\sin(2\pi ft)]. \tag{22}$$

For some conditions, namely, when the magnitudes of f and ϕ^{-1} are comparable, such an oscillation leads to the counterintuitive result that the variance of the particle position increases as the trap stiffness increases.

Stochastic resonance[16] occurs in the presence of a double-well potential subject to an oscillating force of magnitude c and frequency f, such that

$$F(x(t),t) = -ax^3 + bx + c\sin(2\pi ft), \tag{23}$$

where the force oscillation modulates the height of the potential barrier that the particle must overcome to jump to the other potential well. If f is comparable to the Kramers jump frequency, there can be a partial synchronization of the jumps with the oscillating force. This synchronization strongly depends on the temperature of the system. At low temperatures, the particle cannot jump over the potential barrier because the intensity of the noise is not large enough. At

high temperatures, the particle is not significantly affected by the force modulation. Hence, there is an optimal temperature at which the synchronization occurs. A good problem is to find this temperature numerically.

ACKNOWLEDGMENTS

This work was partially supported by the Scientific and Technological Research Council of Turkey (TUBITAK) under Grant Nos. 111T758 and 112T235, and Marie Curie Career Integration Grant (MC-CIG) under Grant PCIG11 GA-2012-321726.

[a]Electronic mail: giovanni.volpe@fen.bilkent.edu.tr

[1]S. H. Strogatz, *Nonlinear Dynamics and Chaos* (Perseus Books, Reading, MA, 1994).
[2]E. Nelson, *Dynamical Theories of Brownian Motion* (Princeton U.P., Princeton, NJ, 1967).
[3]D. Babič, C. Schmitt, and C. Bechinger, "Colloids as model systems for problems in statistical physics," Chaos **15**, 026114-1-6 (2005).
[4]Arthur Ashkin, "Optical trapping and manipulation of neutral particles using lasers," Proc. Natl. Acad. Sci. U.S.A. **94**, 4853–4860 (1997).
[5]Kirstine Berg-Sørensen and Henrik Flyvbjerg, "Power spectrum analysis for optical tweezers," Rev. Sci. Instrum. **75**, 594–612 (2004).
[6]Alexander Rohrbach, Christian Tischer, Dirk Neumayer, Ernst-Ludwig Florin, and Ernst H. K. Stelzer, "Trapping and tracking a local probe with a photonic force microscope," Rev. Sci. Instrum. **75**, 2197–2210 (2004).
[7]Giorgio Volpe, Giovanni Volpe, and Dmitri Petrov, "Brownian motion in a nonhomogeneous force field and photonic force microscope," Phys. Rev. E **76**, 061118-1–10 (2007).
[8]T. T. Perkins, "Optical traps for single molecule biophysics: A primer," Laser Photon. Rev. **3**, 203–220 (2009).
[9]Alexis I. Bishop, Timo A. Nieminen, Norman R. Heckenberg, and Halina Rubinsztein-Dunlop, "Optical application and measurement of torque on microparticles of isotropic nonabsorbing material," Phys. Rev. A **68**, 033802-1–8 (2003).
[10]Arthur La Porta and Michelle D. Wang, "Optical torque wrench: Angular trapping, rotation, and torque detection of quartz microparticles," Phys. Rev. Lett. **92**, 190801-1–4 (2004).
[11]Giovanni Volpe and Dmitri Petrov, "Torque detection using brownian fluctuations," Phys. Rev. Lett. **97**, 210603-1–4 (2006).
[12]B. Øksendal, *Stochastic Differential Equations*, 6th ed. (Springer, Heidelberg, 2003).
[13]P. E. Kloeden and E. Platen, *Numerical Solution of Stochastic Differential Equations* (Springer, Heidelberg, 1999).
[14]Lowell I. McCann, Mark Dykman, and Brage Golding, "Thermally activated transitions in a bistable three-dimensional optical trap," Nature **402**, 785–787 (1999).
[15]Giovanni Volpe, Sandro Perrone, J. Miguel Rubi, and Dmitri Petrov, "Stochastic resonant damping in a noisy monostable system: Theory and experiment," Phys. Rev. E **77**, 051107-1–7 (2008).
[16]Luca Gammaitoni, Peter Hänggi, Peter Jung, and Fabio Marchesoni, "Stochastic resonance," Rev. Mod. Phys. **70**, 223–287 (1998).
[17]Stephen P. Smith, Sameer R. Bhalotra, Anne L. Brody, Benjamin L. Brown, Edward K. Boyda, and Mara Prentiss, "Inexpensive optical tweezers for undergraduate laboratories," Am. J. Phys. **67**, 26–35 (1999).
[18]John Bechhoefer and Scott Wilson, "Faster, cheaper, safer optical tweezers for the undergraduate laboratory," Am. J. Phys. **70**, 393–400 (2002).
[19]D. C. Appleyard, K. Y. Vandermeulen, H. Lee, and M. J. Lang, "Optical trapping for undergraduates," Am. J. Phys. **75**, 5–14 (2007).
[20]See supplemental material at http://dx.doi.org/10.1119/1.4772632 for the Matlab codes and a short introduction.
[21]Scilab < www.scilab.org/>.
[22]J. P. Sethna, *Entropy, Order Parameters and Complexity* (Oxford U.P., Oxford, 2006).
[23]E. M. Purcell, "Life at low Reynolds numbers," Am. J. Phys. **45**, 3–11 (1977).
[24]Tongcang Li, Simon Kheifets, David Medellin, and Mark G. Raizen, "Measurement of the instantaneous velocity of a brownian particle," Science **328**, 1673–1675 (2010).
[25]K. C. Neuman and A. Nagy, "Single-molecule force spectroscopy: optical tweezers, magnetic tweezers and atomic force microscopy," Nat. Methods **5**, 491–505 (2008).
[26]A. Ashkin, J. M. Dziedzic, J. E. Bjorkholm, and Steven Chu, "Observation of a single-beam gradient force optical trap for dielectric particles," Opt. Lett. **11**, 288–290 (1986).
[27]Giovanni Volpe, Jan Wehr, Dmitri Petrov, and J Miguel Rubi, "Thermal noise suppression: how much does it cost?," J. Phys. A: Math. Theor. **42**, 095005-1–8 (2009).
[28]Giorgio Volpe, Giovanni Volpe, and Dmitri Petrov, "Singular-point characterization in microscopic flows," Phys. Rev. E **77**, 037301-1–4 (2008).
[29]F. Borghese, P. Denti, R. Saija, M. A. Iatì, and O. M. Maragò, "Radiation torque and force on optically trapped linear nanostructures," Phys. Rev. Lett. **100**, 163903-1–4 (2008).